Inorg. Chem. **2006**, *45*, 2376–2378

New Valence-Sandwich $[Mn^{II}_4Mn^{III}_4Mn^{II}_4]$ Aggregate Showing Single-Molecule Magnet Behavior

Yangguang Li,[†,‡] Wolfgang Wernsdorfer,[§] Rodolphe Clérac,[||] Ian J. Hewitt,[†] Christopher E. Anson,[†] and Annie K. Powell*[,†]

Institut für Anorganische Chemie, Universität Karlsruhe, Engessserstrasse Geb. 30.45, D-76128 Karlsruhe, Germany, Laboratoire Louis Néel CNRS, 25 Avenue des Martyrs BP166, 38042 Grenoble Cedex 9, France, and Centre de Recherche Paul Pascal, CNRS UPR 8641, 115 Avenue du Dr. A. Schweitzer, 33600 Pessac, France

Received October 21, 2005

The reaction of manganese(II) acetate, 1,1,1-tris(hydroxymethyl)-methane (H_3thme), and triethylamine in methanol leads to the formation of $[Mn_{12}O_2(OMe)_2(thme)_4(OAc)_{10}(H_2O)_4]\cdot 2MeOH$. The $[Mn^{III}_4Mn^{II}_8]$ core consists of a central $[Mn^{III}_4O_6]$ rhombus sandwiched by two $[Mn^{II}_4O_7]$ fragments. Frequency-dependent ac susceptibility and hysteresis loops in the magnetization indicate single-molecule magnet behavior with a pure quantum-tunneling regime of relaxation below 0.2 K.

A bottom-up approach to the synthesis and crystallization of high-nuclearity, magnetically coupled transition-metal aggregates is currently a major focus of research in the area of nanoscale materials.[1] In this field, nanoscale molecules exhibiting single-molecule magnet (SMM) behavior are of special interest owing to their potential applications in data storage and quantum computation as quantum bits.[2,3] Manganese carboxylate aggregates have been a fruitful source of new SMMs in recent years[3a,4] because these clusters include the necessary ingredients of SMMs, i.e., large-spin ground states (*S*) and a large uniaxial anisotropy (*D*) (here arising from the presence of Jahn−Teller distorted Mn^{III} ions), giving rise to the superparamagnetic-like property governed by a barrier to magnetization relaxation. At lower temperatures, this thermally active regime is replaced by quantum tunneling of the magnetization (QTM) that is governed by a small transverse anisotropy term (*E*). Synthetic strategies have therefore concentrated on obtaining aggregates with a high-spin ground state and appropriate magnetic anisotropy (large and small values of *D* and *E* parameters, respectively). The use of tripodal ligands such as 1,1,1-tris(hydroxymethyl)methane (H_3thme) in manganese carboxylate chemistry has been successful in this respect, resulting in the syntheses of $[Mn_2]$,[5a] $[Mn_3]$,[5b] $[Mn_8]$,[5c] $[Mn_9]$,[5d] $[Mn_{12}]$,[5c,e] and $[Mn_{22}]$[5f] SMMs. It is noteworthy that these compounds have been prepared exclusively from the reactions of trinuclear starting materials $[Mn_3O(RO_2)_6(L)_3]^n$ ($n = 0$ or 1+) with tripodal ligands in MeCN or methanol. We are investigating the reactions of simple Mn^{II} salts with a range of carboxylate anions and tripodal ligands in basic methanol solutions in order to explore new routes to Mn aggregates that might show SMM behavior. We describe here a new mixed-valence $[Mn^{III}_4Mn^{II}_8]$ cluster, $[Mn_{12}O_2(OMe)_2(thme)_4(OAc)_{10}(H_2O)_4]\cdot 2MeOH$ (**1**).

The reaction of $Mn(OAc)_2\cdot 4H_2O$ (3 mmol) and the ligand H_3thme (1 mmol) with triethylamine (3 mmol) in MeOH

* To whom correspondence should be addressed. E-mail: powell@chemie.uni-karlsruhe.de.

[†] Universität Karlsruhe.

[‡] Present address: Faculty of Chemistry, Northeast Normal University, Changchun 130024, China.

[§] Laboratoire Louis Néel CNRS.

[||] Centre de Recherche Paul Pascal.

(1) (a) Murugesu, M.; Clérac, R.; Anson, C. E.; Powell, A. K. *Inorg. Chem.* **2004**, *43*, 7269−7271. (b) Murugesu, M.; Clérac, R.; Anson, C. E.; Powell, A. K. *Chem. Commun.* **2004**, 1598−1599.

(2) (a) Leuenberger, M. N.; Loss, D. *Nature* **2001**, *410*, 789−793. (b) Hill, S.; Edwards, R. S.; Aliaga-Alcalde, N.; Christou, G. *Science* **2003**, *302*, 1015−1018.

(3) (a) Sessoli, R.; Tsai, H.-L.; Schake, A. R.; Wang, S.; Vincent, J. B.; Folting, K.; Gatteschi, D.; Christou, G.; Hendrickson, D. N. *J. Am. Chem. Soc.* **1993**, *115*, 1804−1816. (b) Christou, G.; Gatteschi, D.; Hendrickson, D. N.; Sessoli, R. *MRS Bull.* **2000**, *25*, 66−71. (c) Gatteschi, D.; Sessoli, R. *Angew. Chem., Int. Ed.* **2003**, *42*, 268−297.

(4) (a) Wemple, M. W.; Tsai, H.-L.; Folting, K.; Hendrickson, D. N.; Christou, G. *Inorg. Chem.* **1993**, *32*, 2025−2031. (b) King, P.; Wernsdorfer, W.; Abboud, K. A.; Christou, G. *Inorg. Chem.* **2004**, *43*, 7315−7323. (c) Murugesu, M.; Habrych, M.; Wernsdorfer, W.; Abboud, K. A.; Christou, G. *J. Am. Chem. Soc.* **2004**, *126*, 4766−4767. (d) Soler, M.; Wernsdorfer, W.; Folting, K.; Pink, M.; Christou, G. *J. Am. Chem. Soc.* **2004**, *126*, 2156−2165. (e) Tasiopoulos, A. J.; Vinslava, A.; Wernsdorfer, W.; Abboud, K. A.; Christou, G. *Angew. Chem., Int. Ed.* **2004**, *43*, 2117−2121.

(5) (a) Mishra, A.; Wernsdorfer, W.; Parsons, S.; Christou, G.; Brechin, E. K. *Chem. Commun.* **2005**, 2086−2088. (b) Scott, R. T. W.; Parsons, S.; Murugesu, M.; Wernsdorfer, W.; Christou, G.; Brechin, E. K. *Chem. Commun.* **2005**, 2083−2085. (c) Brechin, E. K.; Soler, M.; Christou, G.; Helliwell, M.; Teat, S. J.; Wernsdorfer, W. *Chem. Commun.* **2003**, 1276−1277. (d) Brechin, E. K.; Soler, M.; Davidson, J.; Hendrickson, D. N.; Parsons, S.; Christou, G. *Chem. Commun.* **2002**, 2252−2253. (e) Rajaraman, G.; Murugesu, M.; Sanudo, E. C.; Soler, M.; Wernsdorfer, W.; Helliwell, M.; Muryn, C.; Raftery, J.; Teat, S. J.; Christou, G.; Brechin, E. K. *J. Am. Chem. Soc.* **2004**, *126*, 15445−15457. (f) Murugesu, M.; Raftery, J.; Wernsdorfer, W.; Christou, G.; Brechin, E. K. *Inorg. Chem.* **2004**, *43*, 4203−4209.

10.1021/ic051819m CCC: $33.50
Published on Web 02/11/2006

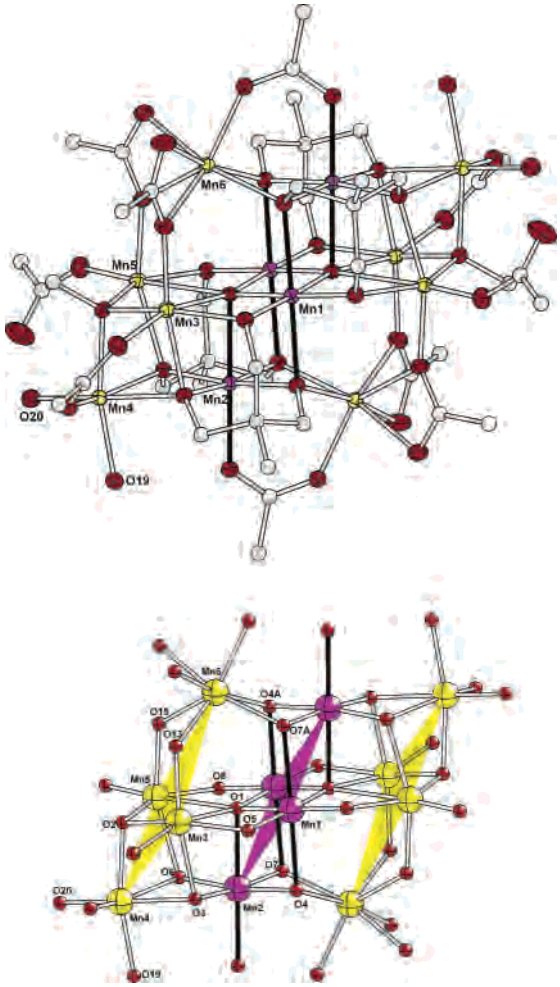

Figure 1. (a) ORTEP representation of the aggregate in **1**, with 50% thermal ellipsoids for Mn and O atoms. H atoms and lattice MeOH molecules have been omitted for clarity. Solid black lines indicate the Mn^{III} Jahn−Teller elongation axes; Mn^{III} ions are in purple, Mn^{II} ions in yellow, O atoms in red, and C atoms in gray. (b) Metal−oxygen core of **1**. The central $[Mn^{III}_4]$ rhombus (purple) is sandwiched by two $[Mn^{II}_4]$ fragments (yellow).

(10 mL) results in the crystallization of **1** after 3 days in ∼60% yield.[6] Complex **1** (Figure 1a) crystallizes in the monoclinic space group $P2_1/n$,[7] and the structure of the aggregate is shown in Figure 1. In the core, all of the Mn ions are six-coordinate except Mn6, which is seven-coordinate. Mn1 and Mn2 can be assigned as Mn^{III}, with the remaining Mn centers as Mn^{II}, based on charge-balance consideration, bond-valence sum calculations,[8] and the Jahn−Teller elongation axes on Mn1 and Mn2 (O4−Mn1−O7′ and O1−Mn2−O11). Notably, all of the elongation axes of the Mn^{III} centers are close to co-parallel. On the basis of the above oxidation states, the mixed-valent $[Mn_{12}O_{20}]$ core can be described as a central rhomboid $\{Mn^{III}_4O_6\}$ layer (Mn1, Mn2, O1, O4, O7, and their symmetry equivalents) sandwiched by two $\{Mn^{II}_4O_7\}$ layers (Mn3, Mn4, Mn5, Mn6, O2, O3, O5, O6, O8, O13, O15, and their symmetry equivalents) (Figure 1b). Such a valence-sandwich-type topology is only the second reported example in Mn aggregates.[10] With the exception of Mn6, which has been pulled out of position by the chelating acetates, the structure of the metal−oxygen core approximates closely to a fragment of the rock salt lattice type.

The two oxo ligands (O1 and O1′) adopt a μ_5-bridging mode, which is still rather unusual in manganese carboxylate aggregates. The methoxo ligands adopt a typical μ_3-bridging mode. The four thme^{3-} ligands are all fully deprotonated, and each of them uses two arms to form μ_3-OR bridges, while the third arm acts as a μ_2 bridge. Of the 10 acetate ligands, 4 form syn,syn bridges, another 4 adopt a less common chelate-bridging mode,[4d] and the remaining 2 bond terminally to Mn^{II} centers (Mn5). The four aqua ligands are coordinated to the peripheral Mn^{II} centers (Mn4). These form H bonds to acetate ligands, either in the same molecule, stabilizing the monodentate acetates, or to acetates in neighboring molecules, forming a planar two-dimensional packing of $[Mn_{12}]$ molecules in the crystal (Figure S1 in the Supporting Information).

Solid-state dc magnetic susceptibility (χ) data were collected in the range 1.8−300 K at 0.1 T (Figure S2 in the Supporting Information). Above 100 K, the magnetic susceptibility follows a Curie−Weiss behavior with $C = 41.5$ cm^3 mol^{-1} K and $\theta = -47$ K. The Curie constant is slightly smaller than the expected value for 4 Mn^{III} and 8 Mn^{II} noninteracting spins (∼47 cm^3 mol^{-1} K for $g = 2$). The negative Weiss constant indicates the presence of dominant antiferromagnetic interactions within the aggregates. The effects of these interactions are also observable on a plot of χT vs T, where χT decreases continuously from 35.4 cm^3 mol^{-1} K at 300 K to 8.2 cm^3 mol^{-1} K at 1.8 K. Even at this temperature, the χT product is still decreasing, indicating that low-lying excited states are still significantly populated (Figures S2 in the Supporting Information). Therefore, fitting of the M vs H/T data cannot be used to determine unambiguously the spin ground state S and the D term of this Mn_{12} complex.

To investigate whether **1** might be a SMM, ac susceptibility measurements were performed in a 3.5-G ac field oscillating at 10−1000 Hz and with a zero applied dc field (Figure 2). The $\chi' T$ product (Figure 2, top) steadily decreases

(6) Calcd for $C_{42}H_{80}O_{40}Mn_{12}$ (i.e., loss of both lattice MeOH): C, 26.77; H, 4.28. Found: C, 26.65; H, 4.45. Selected IR data (KBr, cm^{-1}): 1573vs, 1423vs, 1344m, 1212w, 1121s, 1050s, 1029s, 1000w, 953w, 914w, 674m, 657w, 617m, 579s, 506m, 469s.

(7) Crystal data for **1** ($C_{44}H_{88}Mn_{12}O_{42}$): red-brown block (0.23 × 0.21 × 0.08 mm), $M = 1948.41$, monoclinic, $P2_1/n$, $a = 11.8465(12)$ Å, $b = 14.2914(14)$ Å, $c = 20.564(2)$ Å, $\beta = 96.596(2)°$, $V = 3458.5(6)$ Å^3, $T = 100$ K, $Z = 2$, $D_{calc} = 1.871$ Mg m^{-3}, $F(000) = 1976$, μ(Mo Kα) = 2.207 mm^{-1}. 16 134 data were measured on a Bruker SMART Apex ($4.5 < 2\theta < 56.3°$), of which 7823 were unique ($R_{int} = 0.0297$); semiempirical absorption correction,[11] $T_{max}/T_{min} = 0.901/0.592$. Refinement[12] (466 parameters) to wR2 = 0.1038, $S = 1.007$ (all data), R1 = 0.0398 [6395 data with $I > 2\sigma(I)$]; final difference peak/hole +1.00/−0.74 e Å^{-3}. CCDC 286909.

(8) Liu, W.; Thorp, H. H. *Inorg. Chem.* **1993**, *32*, 4102−4105. Calculated oxidation states for Mn1 and Mn2 are 2.91 and 3.00, respectively, and for Mn3−Mn6 are 1.90−2.07.

(9) Wernsdorfer, W. *Adv. Chem. Phys.* **2001**, *118*, 99−190.

(10) Affronte, M.; Lasjounias, J. C.; Wernsdorfer, W.; Sessoli, R.; Gatesschi, D.; Heath, S. L.; Fort, A.; Rettori, A. *Phys. Rev. B: Condens. Matter Mater. Phys.* **2002**, *66*, 064408/1−064408/7.

(11) Sheldrick, G. M. *SADABS*; University of Göttingen: Göttingen, Germany, 1996.

(12) Sheldrick, G. M. *SHELXTL*, version 5.1; Bruker AXS Inc.: Madison, WI, 1997.

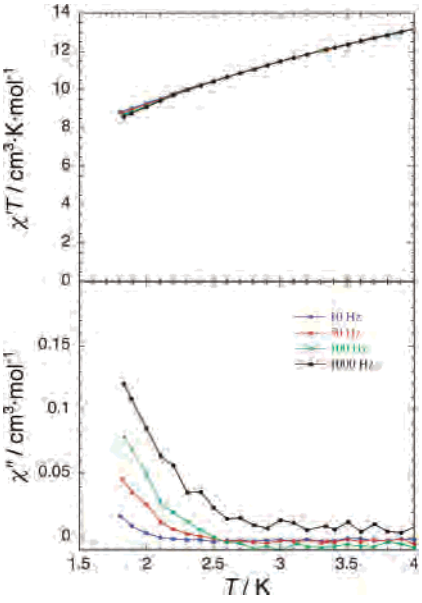

Figure 2. Temperature dependence of the in-phase (χ') (as $\chi'T$, top) and out-of-phase (χ'') (bottom) ac susceptibility in a 3.5-G oscillating field at the indicated frequencies.

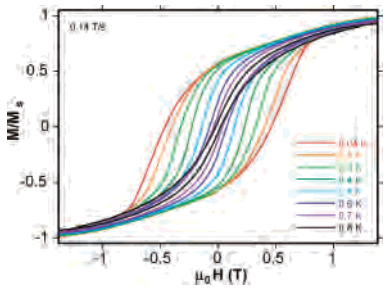

Figure 3. Field hysteresis loops of the normalized magnetization for **1** at a field scan rate of 0.14 T s^{-1} in the temperature range of 0.8−0.04 K.

with decreasing temperature, confirming the population of low-lying excited states. From these data, a rough estimation of the spin ground state can be obtained by extrapolating the plot to 0 K, where only the ground state would be populated. A $\chi'T$ value of ~5 cm^3 mol^{-1} K is found and could indicate a ground state around $S = 2$ or 3.[4b] Although the $\chi'T$ vs T plot shows no obvious frequency dependence above 1.8 K, the χ'' vs T plot (Figure 2, bottom) clearly shows nonzero and frequency-dependent χ'' signals below 3 K, indicating a slow relaxation of the magnetization.

To confirm SMM behavior, measurements of magnetization vs dc field were made on single crystals of **1** using a micro-SQUID apparatus.[9] Hysteresis loops, the characteristic property of a magnet, are indeed observed (Figures 3 and S3 in the Supporting Information). The coercivity is strongly temperature- and time-dependent, increasing with decreasing temperature or increasing field sweep rate, demonstrating the superparamagnetic-like behavior of **1**. The observation of very "rounded" hysteresis loops that do not fully saturate further indicates the presence of very low-lying spin states,

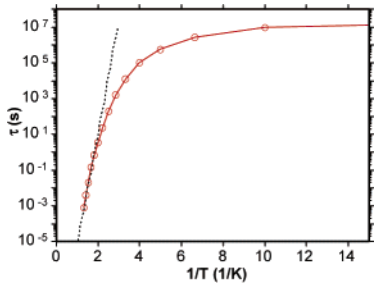

Figure 4. τ vs $1/T$ plot for **1**.

as might be expected given the high Mn^{II} content of **1**. These closely spaced spin levels, together with probable intermolecular interactions in **1** (Figure S1 in the Supporting Information) may well have smeared out the step features (resonant QTM) usually observed on M vs H curves for a SMM. Nevertheless, hysteresis loops become temperature-independent below about 0.2 K (while staying sweep-field-rate-dependent), indicating the presence of a pure quantum regime of magnetization relaxation as expected for SMMs. To determine the relaxation time of this system, magnetization decay data were collected in the 0.04−0.8 K range (Figure S4 in the Supporting Information). For complex **1**, however, the M/M_s vs t curves cannot be fitted by a simple exponential law, and a scaling procedure[10] was applied to extract the temperature dependence of the mean relaxation time $\tau(T)$. The result is shown in Figure 4. Above ca. 0.2 K, the relaxation rate is temperature-dependent. The straight line in Figure 4 is a fit to an Arrhenius law, yielding the values $\tau_0 = 3 \times 10^{-11}$ s and $U_{eff} = 12.7$ K. Below ca. 0.2 K, the relaxation rate becomes temperature-independent, suggesting the occurrence of ground-state QTM, expected for SMM behavior.

In conclusion, complex **1** is a rare example in the manganese carboxylate−tripodal ligand system of an aggregate assembled from simple Mn^{II} ions showing an unusual valence-sandwich structural motif. dc and ac susceptibilities confirm its SMM behavior with hysteresis loops and QTM. Efforts to substitute the acetate anion with other carboxylate ligands (such as $PhCO_2^-$, $Cl_3CCO_2^-$, or $Me_3CCO_2^-$) have led to a series of new Mn clusters, which will be reported later.

Acknowledgment. This work was supported by the DFG (Grant SPP 1137 and the Center for Functional Nanostructures), QuEMolNa (Grant MRTN-CT2003-504880), MAGMANet (Grant NMP3-CT-2005-515767), the Conseil Régional d'Aquitaine, the Université Bordeaux 1, and the CNRS.

Supporting Information Available: Crystallographic details (CIF) for **1** and plots of the packing, χT vs T, and M/M_s vs t for **1**. This material is available free of charge via the Internet at http://pubs.acs.org.

IC051819M